EUROPEAN ORGANIZATION FOR NUCLEAR RESEARCH
CERN – EST

CERN EST/2001-001 (SM)

ELECTRON STIMULATED CARBON ADSORPTION IN ULTRA HIGH VACUUM MONITORED BY AUGER ELECTRON SPECTROSCOPY (AES)

C. Scheuerlein, M. Taborelli

Abstract

Electron stimulated carbon adsorption at room temperature (RT) has been studied in the context of radiation induced surface modifications in the vacuum system of particle accelerators.
The stimulated carbon adsorption was monitored by AES during continuous irradiation by 2.5 keV electrons and simultaneous exposure of the sample surface to CO, CO_2 or CH_4. The amount of adsorbed carbon was estimated by measuring the carbon Auger peak intensity as a function of the electron irradiation time.
Investigated substrate materials are technical OFE copper and TiZrV non-evaporable getter (NEG) thin film coatings, which are saturated either in air or by CO exposure inside the Auger electron spectrometer.
On the copper substrate electron induced carbon adsorption from gas phase CO and CO_2 is below the detection limit of AES. During electron irradiation of the non-activated TiZrV getter thin films, electron stimulated carbon adsorption from gas phase molecules is detected when either CO or CO_2 is injected, whereas the CH_4 partial pressure has no influence on the C-KLL intensity evolution.

Paper submitted for publication to Journal of Vacuum Science and Technology A

Geneva, Switzerland
June 2001

1. INTRODUCTION

Particle induced surface modifications, as they occur on the inner surfaces of accelerator ultra high vacuum (UHV) systems, are advantageous for the operation of accelerators, since they usually decrease surface degassing [1] and secondary electron emission [2] of air exposed metal surfaces. In this context particle stimulated surface modifications are referred to as "conditioning" or "beam scrubbing". In fact, the design luminosity of particle accelerators is often only achieved after a certain conditioning period and the understanding of the conditioning process is therefore important in order to predict the required conditioning time. For CERN's next accelerator, the Large Hadron Collider (LHC), a full conditioning of the internal OFE copper vacuum chamber surfaces is expected [3] after an electron exposure of approximately 10^{-3} C mm^{-2}.

Electron beam induced surface modifications are also known to influence the results of surface analysis techniques, which use electron beams as excitation source. In the terminology of surface analysts these surface modifications are usually referred to as electron beam damage. In AES electron beam damage [4] can become detectable, for instance, by a modification of oxygen and carbon peak intensities after primary electron (PE) exposures between 10^{-5} and 10^{-3} C mm^{-2}.

Besides other phenomena, such as the decomposition and/or desorption of adsorbed species, electron beam induced surface modifications can include the stimulated deposition of gas-phase components. This phenomenon is exploited in the microelectronics industry in order to produce three-dimensional structures on nm scales [5]. Deposition rates in the order of 1 nm per second can be obtained by the injection of, for instance, metal carbonyls into the deposition system, in which very high gas densities above the substrate can be achieved by means of a differential pumping system. Another important application of electron stimulated deposition is the production of tips for atomic force microscopes [6]. This note deals with the phenomenon of electron stimulated carbon adsorption in UHV, with CO, CO_2 and CH_4 as the only carbon containing molecules which are present in the residual gas.

Due to its high sensitivity for elements with low atomic number and because of its surface sensitivity AES should be ideally suited for the study of electron stimulated carbon adsorption. Moreover, the same electron beam can be used simultaneously for the generation of Auger electrons and for stimulating gas phase adsorption. An electron stimulated adsorption from C-containing gas phase molecules has been observed by AES on Ni(110) [7, 8], various TiO_2 surfaces [9, 10], Al(111) [11] and ZnS [12]. On the other hand a CO, CO_2 and CH_4 pressure independent electron stimulated carbon growth rate is reported on sputter-cleaned polycrystalline copper [13].

In the present study two materials that may be used for the construction of accelerator UHV systems, notably chemically polished OFE copper and a TiZrV non-evaporable getter (NEG) thin film, are investigated. Electron stimulated carbon deposition is studied in an Auger electron spectrometer during continuous electron irradiation and a simultaneous exposure of the substrate surface to either CO, CO_2 or CH_4.

2 EXPERIMENTAL

The only experimental parameters that are changed during the measurements described below are the CO, CO_2 and CH_4 partial pressures and the sample materials. All other experimental settings are kept constant.

2.1 Data acquisition

The AES measurements were carried out with a special Auger electron spectrometer, which is described in detail in reference 14. The single-pass cylindrical mirror analyzer (PHI 15-110B) has a relative energy resolution, $\Delta E/E$, of 1.2 % (full width at half-maximum).

The total base pressure before the surface treatments is 10^{-9} mbar (N_2 equivalent), H_2 being the dominant gas species followed by water vapour (~ $2 \cdot 10^{-10}$ mbar). Before gas injection the partial pressures of CO, CO_2 and CH_4 are all in the order of 10^{-10} mbar and no other carbon containing molecules are detected in the residual gas. For gas exposures the chosen gas is admitted to the vacuum system via an automatically regulated variable leak valve. The gas purity is controlled by means of a residual gas analyzer and the injection pressure is measured with a non calibrated Penning gauge (Balzers type IKR U70).

The electron exposures are carried out with a static electron beam, which is provided by the thermionic electron gun used to excite core electrons for AES. During the continuous electron irradiation Auger spectra are periodically acquired.

The direct EN(E) Auger spectra are acquired with a 1 eV step. The primary electron (PE) energy is 2.5 keV and the PE beam current is typically 1 μA, incident normal to the sample surface. The minimum electron dose that is accumulated during a single AES measurement is 10^{-3} C mm^{-2} and the maximum electron dose, to which the investigated surfaces are exposed, is 1 C mm^{-2}.

2.2 Data processing

Since the elements that are detected on the investigated surfaces are not uniformly distributed in the analyzed volume, a calculation of relative concentrations is avoided. Instead the evolution of the absolute Auger peak intensities is monitored in order to determine the degree of carbon uptake during the surface treatments.

The use of absolute peak intensities requires a normalization of the Auger spectra in order to reduce the influence of instrumental parameters, such as fluctuations of the PE current and the detector efficiency. In particular the amplification of the secondary electron multiplier (channeltron) shows a systematic decrease with the acquisition time when the channeltron voltage is kept at 1 keV.

For the normalization all direct EN(E) spectra are multiplied by a constant factor so that the background intensity value at 600 eV of all spectra equals a certain value. The background intensity at 600 eV is averaged over an energy range of 20 eV in order to reduce the effect of noise. For chemical state analysis the normalized EN(E) spectra are numerically differentiated.

The Auger peak areas after subtraction of a linear background are taken as a measure for peak intensity. The comparison of the C-KLL peak area and p-t-p height measurements in Figure 1 shows that the peak area measurement in the direct EN(E) spectra is important for the detection of electron stimulated C adsorption by AES since the C-KLL p-t-p height variations in the derivative spectra are obscured by strong line shape changes [15] during the reported surface treatments.

Both effects, the C-KLL peak shape changes and the detector efficiency fluctuations together would indicate an apparent reduction of the C-KLL peak intensity with increasing irradiation time if the peak intensity were be defined as the p-t-p height in the non-normalized dEN(E)/dE spectra.

The linear background is taken for its simplicity and does not represent the true background shape. It is however assumed that the systematic error caused by the deviation of the linear background signal from the true background for a certain Auger peak is similar on all described surfaces. For C-KLL and O-KLL the linear background is subtracted from 200 eV to 285 eV and 499 eV to 518 eV, respectively.

The sensitivity for carbon is estimated as 400 C-KLL peak intensity units per monolayer (ML). This sensitivity factor has been obtained by saturating a sputter-cleaned Zr surface with CO (with identical experimental parameters as those used during the reported measurements).

For the present study a saturation ML coverage of approximately 10^{15} molecules cm^{-2} is estimated, taking into account a certain degree of surface roughness.

The O-KLL intensity values which are reported in this paper have been scaled so that 400 units correspond also with 1 ML oxygen (again determined by saturating an atomically clean Zr surface by CO). These sensitivity factors are only valid for C and O, which are present on the outermost surface layer. If carbon or oxygen are distributed in depth the AES sensitivity decreases due to the attenuation of the characteristic Auger electrons by overlying material.

The sensitivity factors must be regarded as rough estimates, which are affected by several uncertainties, such as the influence of surface roughness on the ML capacity and the influence of the sample matrix [16] on the C-KLL and O-KLL intensities.

2.3 The samples

The two investigated sample materials are OFE bulk copper and TiZrV non evaporable getter (NEG) thin films. Both materials may be used as the internal surface of particle accelerator UHV systems.

The TiZrV NEG coatings with a thickness of approximately 1 μm are deposited onto stainless steel 316LN by magnetron sputtering. Scanning electron microscope images reveal that the coatings are smooth on a microscopic scale. For more information about the NEG thin film coatings see reference 17. After deposition the TiZrV coating was exposed to air for about 1 h. AES measurements as a function of electron dose have been carried out on as-received (non activated) samples and on TiZrV samples that were activated during several hours at 350 °C and afterwards saturated under vacuum with 3000 L CO.

The OFE copper samples are chemically polished [18] in a solution of sulfamic acid, hydrogen peroxide n-butanol and ammonium citrate. The air exposure time between the chemical treatment and the introduction of the samples into the experimental UHV system is less than 1 h. The copper samples obtained after this treatment are referred to as “technical copper”.

3. RESULTS

3.1 Influence of continuous electron irradiation at various pressures on the surface composition of an in-situ activated TiZrV NEG sample after saturation with CO

Auger peak intensity profile around the irradiated surface area

An in-situ activated TiZrV sample was saturated with 3000 L CO and afterwards irradiated by 10^{-6} A of 2.5 keV electrons at a CO pressure of 10^{-7} mbar. After an irradiation time of 130 min the sample was displaced in 0.05 mm steps and after each step an Auger electron spectrum was acquired. The C-KLL, O-KLL and Zr-MNN peak intensities as a function of the sample position with respect to the centre of the previously irradiated surface area are shown in Figure 2.

The Zr-$M_{45}N_{23}N_{23}$ peak at 92 eV is chosen to represent the metals on the surface because it is the Zr Auger peak which is least affected by changes in oxidation state [19] and due to the low kinetic energy it is also the most surface sensitive metal peak.

The C-KLL area increase and the corresponding Zr signal depletion are consequences of the addition of carbon onto the analyzed surface by the interaction with the electron beam. The oxygen intensity on the irradiated sample area is higher than it is outside this area, indicating the deposition of oxygen during the electron irradiation process. However, the O-KLL intensity in the beam center is lower than the O-KLL intensity at the beam edge, which shows that either

the composition and/or the structure of the deposited layer varies over the irradiated sample area. A similar oxygen distribution over the irradiated surface area has been measured on Ni(110) surfaces after intense electron irradiation and simultaneous CO exposure [8].

From the C-KLL intensity variations in Figure 2 a PE beam diameter of approximately D_{beam} = 0.15 mm at FWHM beam intensity has been estimated.

Peak intensity variation as a function of irradiation time during 10^{-7} mbar CO injection

In Figure 3 the direct EN(E) Auger electron spectra of a TiZrV thin film (activated and saturated with CO) are shown after different electron irradiation times during simultaneous CO injection at 10^{-7} mbar.

The C-KLL intensity increases continuously with irradiation time and the carbon line shape, which is initially carbidic, shows an increasing contribution of graphite [15]. The O-KLL intensity shows initially a slight increase and after 10 min it starts to slowly decrease with irradiation time. The metal peaks are progressively attenuated with increasing electron exposure, indicating a continuous growth of the carbon layer on top of the NEG substrate. Due to the low kinetic energy, the Zr-MNN signal shows the strongest attenuation. The Cl peak, which is present initially, disappears, probably because of electron stimulated desorption (ESD).

Influence of the CO, CO_2 and CH_4 pressure on the rate of C-KLL intensity increase

In Figure 4 the C-KLL peak area variation during electron irradiation of a TiZrV NEG surface (activated and saturated with CO) is plotted as a function of irradiation time at a total pressure of 10^{-9} mbar and during CO, CO_2 or CH_4 injection. All gases were injected at a pressure of 10^{-7} mbar and in addition CO was injected at 10^{-8} mbar.

When no gas is admitted to the Auger spectrometer vacuum system the C-KLL peak area increases linearly with irradiation time. The rate of carbon deposition on the irradiated surface area is in the order of 10^{-3} ML per minute.

The C-KLL intensity increase during the irradiation of TiZrV becomes much faster if CO or CO_2 are injected whereas the CH_4 pressure has no influence on the rate of the C-KLL intensity variation. This clearly shows that an electron stimulated adsorption of carbon from gas phase CO and CO_2 molecules takes place. During CO_2 injection the effect is somewhat delayed with respect to the case of CO.

The higher the CO pressure in the experimental chamber the higher is the rate with which carbon is deposited on the irradiated sample area. During the first 10 min of irradiation at 10^{-7} mbar CO the carbon deposition rate is approximately $2 \cdot 10^{-2}$ ML min^{-1} and with increasing irradiation time the carbon deposition rate decreases.

3.2 Influence of alternating electron and CO exposure on the surface composition of an in-situ activated TiZrV NEG sample after saturation with CO

Alternating electron and CO exposures where performed in order to better understand the mechanism of the pressure dependent electron stimulated carbon adsorption. For this purpose an in-situ activated TiZrV sample was saturated with CO and afterwards exposed to about 10^{-2} C mm^{-2} of 2.5 keV electrons at a total pressure of 10^{-9} mbar. At the end of the electron exposure (corresponding with an irradiation time of 10 min) an Auger spectrum was acquired and then the sample was exposed to 1000 L of CO (100 s CO injection at 10^{-5} mbar) without electron irradiation. Immediately after the gas exposure an Auger spectrum was acquired. This procedure was repeated several times. The C-KLL, O-KLL and Zr-MNN Auger peak intensity variations during the alternating electron and CO exposure are shown in Figure 5.

During the electron irradiation at 10^{-9} mbar the C-KLL intensity remains almost unchanged while the O-KLL intensity decreases significantly due to ESD of oxygen. At the same time the Zr-MNN intensity augments, also indicating the removal of surface material by ESD. After CO exposure the C-KLL and O-KLL peak areas are significantly increased due to the adsorption of CO. Subsequent irradiation decreases the O-KLL intensity, while the carbon intensity is much less affected.

3.3 Influence of continuous electron irradiation and CO_2 exposure on the surface composition of an air exposed NEG surface

In Figure 6 the C-KLL and O-KLL Auger peak area variations as a function of electron irradiation time at different pressures (without gas injection at a total pressure $p_{tot} = 10^{-9}$ mbar and during CO_2 injection at 10^{-7} mbar) are shown for an as-received (air exposed) TiZrV thin film.

The C-KLL intensity evolution on the air exposed NEG surface is similar to that on the in-situ activated and saturated NEG surface. A linear C-KLL increase with irradiation time, corresponding to a carbon deposition rate of about $2 \cdot 10^{-3}$ ML min^{-1}, is observed when no gas is injected ($p_{tot} = 10^{-9}$ mbar). During CO_2 injection at 10^{-7} mbar the carbon deposition rate is initially about 1 order of magnitude faster and slows down with increasing carbon coverage.

The O-KLL area becomes smaller with irradiation time, indicating ESD of oxygen. During CO_2 exposure the oxygen signal depletion is weaker than it is during electron irradiation without gas injection. This shows that the O-KLL peak intensity evolution is the result of a simultaneous ESD and oxygen deposition process.

Some chemical information can be extracted from the Zr-MNN and the C-KLL peaks in the derivative Auger spectra, which are shown in Figure 7. The peak shape and intensity of the Zr-$M_{4,5}N_{2,3}$V peak at 147 eV changes strongly when metallic Zr becomes oxidized. During the oxidation a new peak appears about 7 eV below the peak from unoxidized Zr [20]. Mainly this peak is seen in the Auger spectra of an air exposed TiZrV surface, whereas only a small peak at 147 eV is observed.

During the continuous electron irradiation of the air exposed TiZrV coating, the metallic Zr peak at 147 eV increases at the expense of the peak characteristic for Zr in ZrO_2. This indicates a reduction of ZrO_2 by the electron beam, which is consistent with the depletion of the O-KLL intensity (see Figure 6). From the Ti and V Auger peaks changes in oxidation state can not be detected because of the low energy resolution of the used CMA ($\Delta E/E = 1.2$ %).

On the as received getter sample the C-KLL peak shape is characteristic for graphite. During irradiation the peak shape changes and becomes partly carbidic, which is also an indication that the getter surface becomes more reactive during the electron exposure. If CO_2 is injected during irradiation the growing C-KLL peak does not change its shape, which remains typical for graphite.

3.4 Influence of continuous electron irradiation and CO and CO_2 pressure on the surface composition of technical Cu

Identical measurements as those described above for saturated TiZrV samples were carried out on technical copper. In Figure 8 the C-KLL variation on the technical Cu substrate during PE irradiation at a total pressure of 10^{-9} mbar or during simultaneous injection of either CO or CO_2 at 10^{-7} mbar is shown. The C-KLL peak area values are somewhat decreased after 2 min electron irradiation, indicating ESD of carbon containing molecules. Afterwards the C-KLL peak area increases linearly with irradiation time.

With the estimated intensity value of 400 units for 1 ML adsorbed carbon the rate at which the amount of carbon on the irradiated surface area increases is in the order of 10^{-3} ML min^{-1}. The rate at which the C-KLL intensity increases is independent of the CO and CO_2 partial pressures and, hence, in UHV the electron stimulated C adsorption from gas phase molecules on Cu is, at RT, below the detection limit of AES.

4. DISCUSSION

The impinging electron beam can have an effect on the carbon deposition process by the dissociation of physisorbed molecules and/or influence the adsorption process through a modification of the sample surface. In the following the first case is referred to as electron beam induced deposition (EBID) while the process that requires an electron induced surface modification to occur is called electron stimulated adsorption (ESA).

4.1 Mechanism of the EBID process

Residual gas molecules which impinge on a solid surface have a certain probability to be adsorbed and to remain on the surface for a certain time, the so-called mean sojourn time. During this period the surface molecules can be dissociated by the interaction with PE and SE, which transforms them into non-volatile species that are practically permanently adsorbed on the surface, and into volatile species that are desorbed into the gas phase.

The number of molecules that are dissociated on the sample surface per time dN_{dis} / dt is proportional to the density of reversibly adsorbed molecules per irradiated surface area N, the electron current density f and the dissociation cross section q [1] for the adsorbed molecule at the corresponding electron energy [21].

$$\frac{dN_{dis}}{dt} = N \cdot f \cdot q \qquad \textbf{(1)}$$

The equilibrium surface density N_E of reversibly adsorbed molecules during continuous electron irradiation can be calculated with equation (2) [22]

$$N_E = N_0 \cdot \frac{(g \cdot Z / N_0)}{(g \cdot Z / N_0) + 1/\tau + q \cdot f} \qquad \textbf{(2)}$$

with the sticking coefficient of the gas phase molecules on the substrate surface g, the rate with which the molecules impinge on the substrate surface Z, the molecule density in a complete monolayer N_0, and the mean sojourn time of the non dissociated molecule τ. At RT the mean sojourn time of physisorbed CO and CO_2 is in the order of $\tau = 10^{-11}$ s [23].

Using equation (2) and the experimental parameters, as they were used during the described experiments the equilibrium coverage can be estimated for CO molecules, which are physisorbed at RT, as $N_E = 150$ cm^{-2}. For this estimation a sticking coefficient of g = 0.5 and a monolayer capacity $N_0 = 10^{15}$ cm^{-2} are assumed. The impinging rate of CO molecules at a CO pressure of 10^{-7} mbar at RT is $Z = 2.9 \cdot 10^{13}$ $cm^{-2} \cdot s^{-1}$.

By setting N in equation (1) equal to $N_E = 150$ cm^{-2} the calculated dissociation rate of reversibly physisorbed CO molecules is in the order of $dN_{diss}/dt \approx 10^3$ min^{-1} cm^{-2} (with $f = 3 \cdot 10^{16}$ $cm^{-2} \cdot s^{-1}$ and $q = 10^{-17}$ cm^2). This rate is so low that even after several hours of electron

[1] The onset energy for CO dissociation is 11.2 eV and the maximum cross section for CO dissociation by electron impact $q_{maxCO} = 7.5 \cdot 10^{-17}$ cm^2, obtained at electron energies between 39 and 59 eV. For the present study a dissociation cross section of $q = 10^{-17}$ cm^2 is estimated for the 2.5 keV PE and the contribution of SE with an energy above 11.2 eV is in this estimation neglected.

irradiation the quantity of adsorbed carbon is many orders of magnitude below the detection limit of AES.

4.2 EBID on technical copper surfaces

The CO and CO_2 partial pressures in UHV have no measurable influence on the C-KLL peak intensity evolution on a technical copper surface at RT. Similar results have been obtained on sputter cleaned copper surfaces during electron irradiation and simultaneous injection of either CO, CO_2 or CH_4 [13]. Thus, EBID of carbon from gas phase molecules on copper is in UHV below the detection limit of AES. This is in agreement with above EBID calculations, which show that the dissociation rate on the copper surface at a CO pressure of 10^{-7} mbar is only in the order of $dN_{diss}/dt \approx 10^3$ min^{-1} cm^{-2}.

The reason for the constant, pressure independent carbon deposition, at a rate of approximately 10^{12} molecules min^{-1} cm^{-2}, cannot be explained by the presented measurements. An electron stimulated adsorption from gas phase molecules can be excluded since all possible mechanisms give rise to a pressure dependent deposition rate. A possible explanation could be the deposition of carbon-containing radicals or ions, which are produced at a constant rate by the electron beam through ESD from aperture surfaces inside the electron gun. Such species would only be deposited onto the sample area which is in line of sight with the electron gun opening.

4.3 The ESA mechanism on saturated TiZrV getter surfaces

In the following considerations it is assumed that localised substrate heating by the electron beam is negligible. The localised sample temperature increase under the experimental conditions has been estimated according to Pittaway [24] as less than 1 °C, using the thermal conductivity, density and specific heat of zirconium.

On saturated TiZrV surfaces a carbon deposition from gas phase CO and CO_2 is observed at RT. After 3 - 4 hours irradiation and simultaneous gas exposure at 10^{-7} mbar CO or CO_2 approximately 1 ML of carbon is adsorbed on an activated and saturated TiZrV surface.

From equation (2) it follows that, in ultra high vacuum, EBID from CO and CO_2 molecules occurs at such a low rate that it can not be detected by AES (at RT). Hence, there must be another mechanism by which the electron stimulated carbon adsorption takes place on the saturated getter surface.

The electron irradiation modifies the saturated NEG surfaces in such a way that they can form stronger bonds with CO and CO_2. The CH_4 pressure has no influence on the rate of the C-KLL intensity variation during continuous electron irradiation of getter surfaces, which is explained by the fact that CH_4 molecules are not pumped by NEG at RT [25].

Electron induced defect creation is indicated by the Zr-MNV peak shape changes (Figure 7) and the O-KLL signal depletion during electron irradiation of air exposed TiZrV. These features show that at least ZrO_2 is reduced by the electron beam. Previous studies have shown that adsorption energies are higher on defect positions than they are on ideal surfaces [26].

The fact that on the air exposed NEG the amount of carbon increases, whereas the amount of oxygen decreases, during electron irradiation is a clear indication that the CO and CO_2 molecules are dissociated on the NEG surface. However, the alternating electron and CO exposure measurements show that the electron induced surface defects on the initially saturated NEG are sufficient for the chemisorption of CO. The subsequent electron radiation is then required for the creation of new surface defects, which allow the CO adsorption to proceed. In this way the ESA process on saturated getters differs from the EBID mechanism for simple physisorption, which requires the dissociation of the physisorbed molecules leading to their permanent adsorption.

The rate of electron stimulated carbon adsorption at a CO or CO_2 pressure of 10^{-7} mbar decreases with increasing carbon coverage, and after about 3 h irradiation time, it approaches the rate that is observed during electron irradiation at a total pressure of 10^{-9} mbar. This indicates that the adsorbed carbon layer is less reactive than the NEG substrate (from the C-KLL peak shape evolution it appears that the adsorbed carbon is mainly in the form of graphite). One can therefore expect that, unlike EBID, the ESA process stops when a certain surface coverage of the adsorbate is obtained.

When no gas is injected into the experimental chamber the C-KLL intensity on the saturated TiZrV surface increases linearly with electron irradiation time. Since on the copper surface a similar rate of carbon uptake is observed it is likely that the reason for the linear C-KLL intensity increase is in both cases the same.

4.2 The relevance of electron stimulated carbon adsorption for the conditioning of particle accelerators and for surface analysis measurements by AES

Electron stimulated carbon adsorption during the operation of particle accelerators

On the internal surfaces of copper UHV equipment in accelerators, which are operated at RT, an electron beam deposition of carbon is not expected. However, from equation (2) it follows that the sample temperature has an important influence on the EBID rate, since the equilibrium surface density N_E depends strongly on the mean sojourn time τ. If τ were, for instance, raised to 0.1 s by cooling the substrate, about 0.2 ML of carbon per minute could be continuously deposited at a CO pressure of 10^{-7} mbar under the same experimental conditions as those described above.

Hence, on internal copper surfaces of UHV systems, which are kept at cryogenic temperatures, a continuous electron beam carbon deposition may occur with a significant rate if the relevant partial pressures and the electron current density are sufficiently high. Such conditions may, for instance, be met during a resonant electron multiplication process (multipacting) in copper coated auxiliary equipment of superconducting radio frequency cavities for particle acceleration [27]. In such equipment, the electron beam deposition of carbon might be one reason for the strong change of surface properties, such as the change of the secondary electron yield.

On getter surfaces an electron stimulated carbon adsorption may occur at RT, but in this case the deposition rate will strongly slow down after the adsorption of approximately 1 ML of carbon. If the saturated getter is cooled, EBID can proceed in the same way as it occurs on a cold copper surface.

Artefacts in AES caused by electron stimulated adsorption

When Auger spectra are acquired in a reasonable time electron beam damage through EBID is negligible, while ESD can cause significant variations of the surface composition.

The defects, which are created during an AES analysis, can make a saturated getter surface active, so that it can adsorb residual gas molecules. Therefore, if a previously irradiated surface area is analyzed again after it has been stored for certain time in the experimental vacuum chamber, a markedly different surface composition compared to that of the as-received (non irradiated) surface may be observed. The rate of residual gas adsorption subsequent to the electron beam damage depends on the substrate material, the number of created defects and the residual gas pressure and composition.

5. CONCLUSION

The carbon deposition rate from carbon containing gas species that is induced by an electron beam impinging on the surface depends crucially on the properties of the substrate material.

On copper vacuum chambers that are operated at RT, the electron beam induced deposition of carbon from gas phase CO and CO_2 is negligibly small (below the detection limit of AES). However, at cryogenic temperatures, at which accelerator copper equipment is often used, a significant electron beam induced carbon deposition rate may occur.

On a TiZrV getter that is either saturated by the injection of a large quantity of CO or by an air exposure, electron stimulated adsorption of carbon is observed when the residual gas contains either CO or CO_2, while the CH_4 pressure has no influence on the carbon deposition rate. The creation of defects by the electrons impinging on the surface is sufficient to stimulate the adsorption of CO and CO_2. During the subsequent dissociation of the adsorbed molecules by the electron beam, carbon remains on the surface while most of the oxygen is removed from the surface.

ACKNOWLEDGEMENTS

The TiZrV thin film samples were produced by Pedro Costa Pinto from CERN, EST-SM.

REFERENCES

1 M. Andritschky, Vacuum **39**, (1989), 649-652

2 V. Baglin, B. Henrist, N. Hilleret, E. Mercier, C. Scheuerlein, CERN-SL-2000-007 DI, (2000), 130

3 N. Hilleret et al., CERN, LHC Project Report 290, (1999)

4 C.G. Pantano, T.E. Madey, Application of Surface Science **7** (1981), 115-141

5 H.W.P. Koops, R. Weiel, D.P. Kern, J. Vac. Sci. Technol. B **6**(1), (1988), 477-481

6 K. I. Schiffmann, Nanotechnology **4**, (1993), 163-169

7 H.H. Maden, G. Ertl, Surf. Sci. **35**, (1973), 211-226

8 J. Verhoeven, J. Los, Surf. Sci. **82**, (1979), 109-119

9 A. J. M. Mens, O. L. J. Gijzeman, Appl. Surf. Sci. **99**, (1996), 133-143

10 H.J. Hopman, J. Verhoeven, J.J. Scholtz, R. Fastenau, Appl. Surf. Sci. **111**, (1997), 270-275

11 S.A. Flodström, C.W.B. Martinsson, Applications of Surface Science **10**, (1982), 115-123

12 Y. Darici, P.H. Holloway, J. Sebastian, T. Trottier, S. Jones, J. Rodriquez, J. Vac. Sci. Technol. A **17**(3), (1999), 692-697

13 A. Septier, P. Lebon, J.P. Lachanne, Proceedings of the X International Symposium on Discharge and Electrical Insulation in Vacuum, Columbia, SC, (1982), 89-94

14 C. Benvenuti, R. Cosso, J. Genest, M. Hauer, D. Lacarrere, A. Rijllart, R. Saban, Rev. Sci. Instr. **69**, No. 8, (1996)

15 T.W. Haas, J.T. Grant, G.J. Dooley, J. Appl. Phys. **43**, (1972), 1853

16 H.E. Bishop, Scanning Electron Microscopy, AMF O'Hare, (1984)

17 C. Benvenuti, J.M. Cazaneuve, P. Chiggiato, F. Cicoira, A. Escudeiro Santana, V. Johanek, V. Ruzinov, J. Fraxedas, Vacuum **53**, (1999), 219

18 S. Calatroni et al., Proceedings of the 6th workshop on Radio-frequency Superconductivity, Newport News, VI, USA, (1993)

19 M. Tomita, T. Tanabe, S. Imoto, Surf. Sci. **209**, (1989), 173

20 B. Jungblut, G. Sicking, T. Papachristos, Surf. Interf. Anal. **13**, (1988), 135

21 P.C. Cosby, J. Chem. Phys. **98**(10), (1993), 7804

22 V. Scheuer, H. Koops, T. Tschudi, Microelectronics Engineering **5**, (1986), 423-430

23 J.M. Lafferty, *Foundations of Vacuum Science and Technology*, (John Wiley & Sons, Inc., New York, 1998), 551

24 L.G. Pittaway, Brit. J. Appl. Phys. **15**, (1964), 967

25 J.P. Hobson, R. Chapman, J. Vac. Sci. Technol. A**4**(3), (1986), 300-302

26 T. Bredow, K. Jung, Surf. Sci. **327**, (1995), 398-408

27 H. Lengeler, in *CERN Accelerator School Fifth General Accelerator Physics Course*, edited by S. Turner, (1994), 791

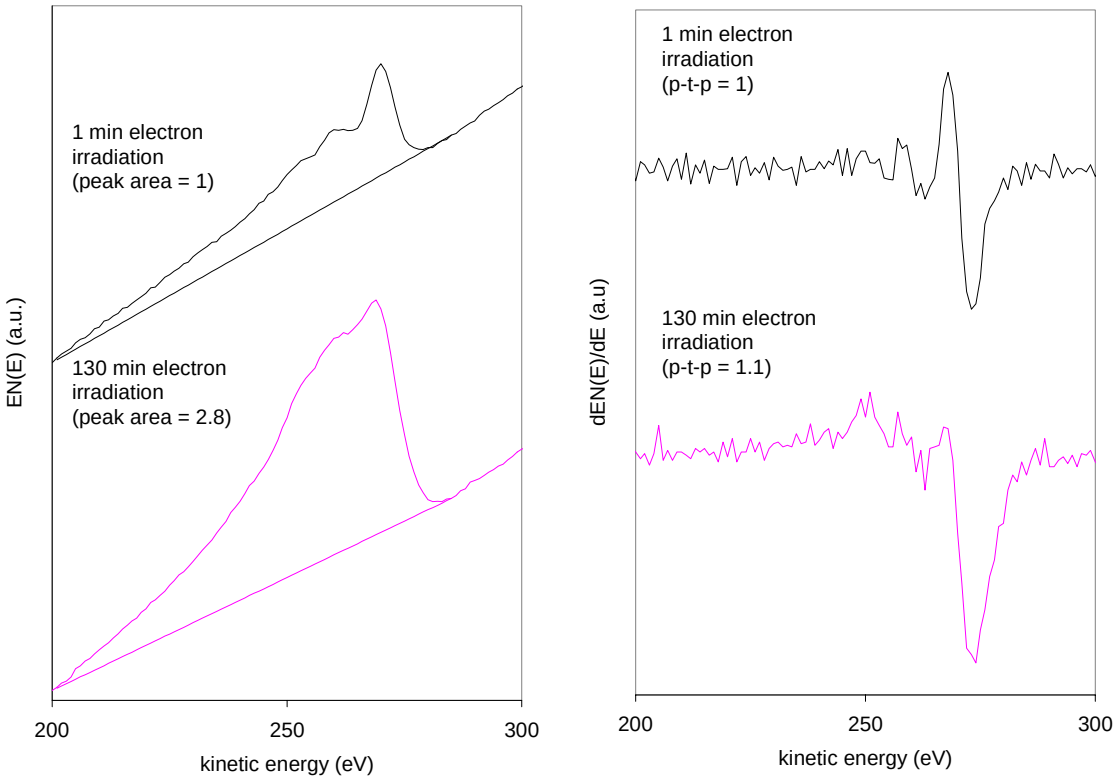

Figure 1: Carbon KLL Auger peaks before and after 130 min electron irradiation of TiZrV at a CO pressure of 10^{-7} mbar. Prior to the electron exposure the TiZrV surface was fully activated and then saturated with 3000 L CO. The EN(E) spectra (left graph) are normalised at the 600 eV background signal and afterwards numerically differentiated (right graph). The peak area is determined after subtraction of a linear background from 200 to 285 eV. The relative increase of the C-KLL intensity by a factor of 2.8 can only be detected from peak area measurements.

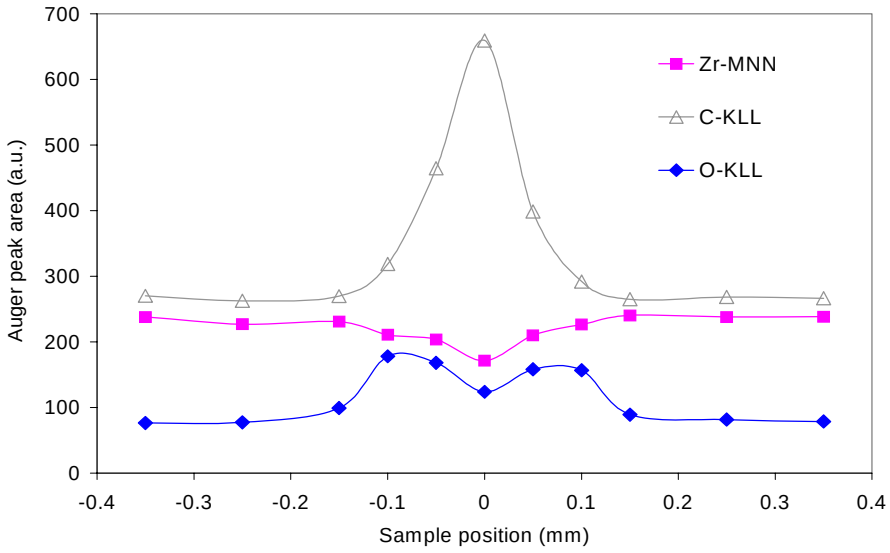

Figure 2: Auger peak areas (Zr-$M_{45}N_{23}N_{23}$, O-KLL, C-KLL) as a function of the sample position around the sample spot which was irradiated during 130 min at a CO pressure of 10^{-7} mbar. The sample is an activated TiZrV NEG, which was saturated with 3000 L CO prior to electron exposure.

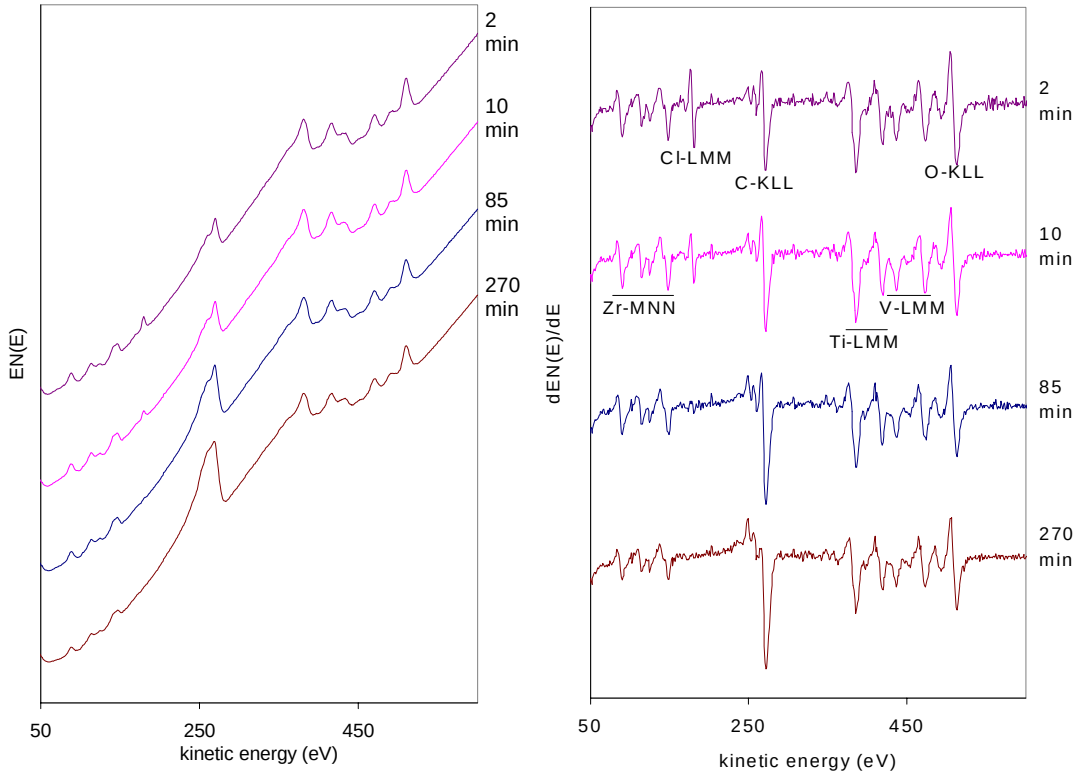

Figure 3: Direct EN(E) (left plot) and derivative dEN(E)/dE Auger spectra of a TiZrV thin film, after different electron irradiation times and a simultaneous CO injection at a pressure of 10^{-7} mbar following an in-situ activation and saturation with 3000 L CO.

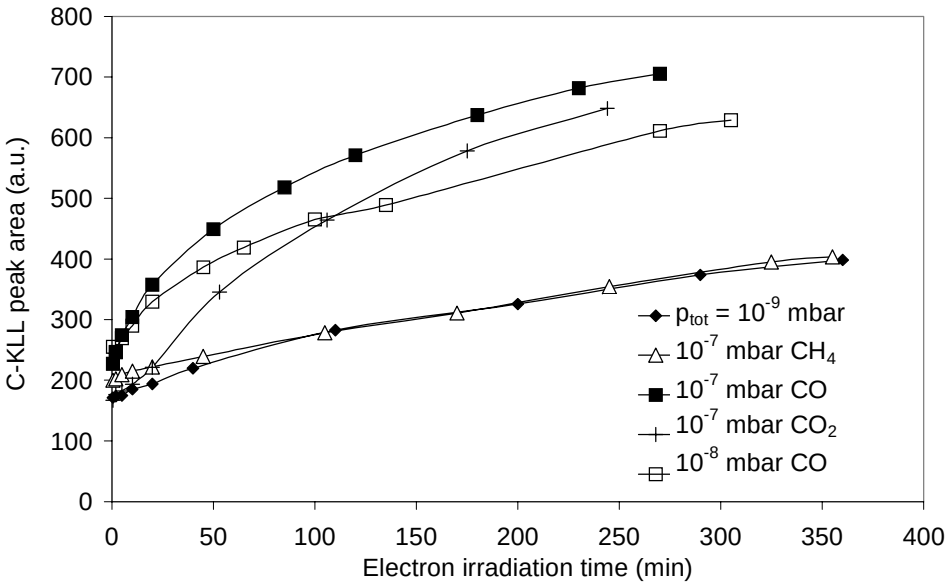

Figure 4: Variation of the C-KLL intensity as a function of irradiation time on a TiZrV sample, which was activated and saturated with 3000 L CO. The PE current is 10^{-6} A and the PE beam area is approximately 0.02 mm^2. The total N_2 equivalent pressure in the vacuum chamber before CO injection is 10^{-9} mbar with CO and CO_2 partial pressures of about 10^{-10} mbar.

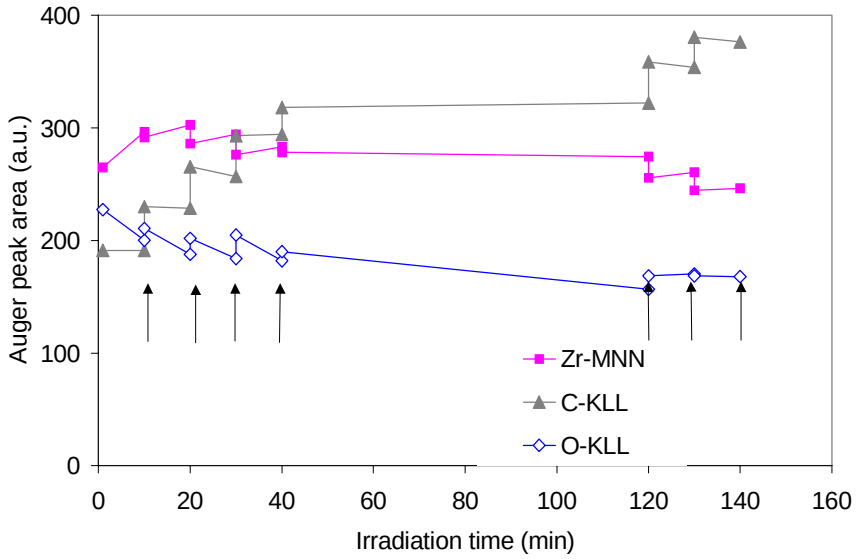

Figure 5: Variation of the Zr-MNN, C-KLL and O-KLL intensity during alternating electron and CO exposure. During electron irradiation the total pressure is 10^{-9} mbar. 10 min of electron irradiation correspond to approximately 10^{-2} C/mm^2. The arrows indicate exposures of 1000 L CO (100 s CO injection at 10^{-5} mbar), which are carried out with the electron beam switched off.

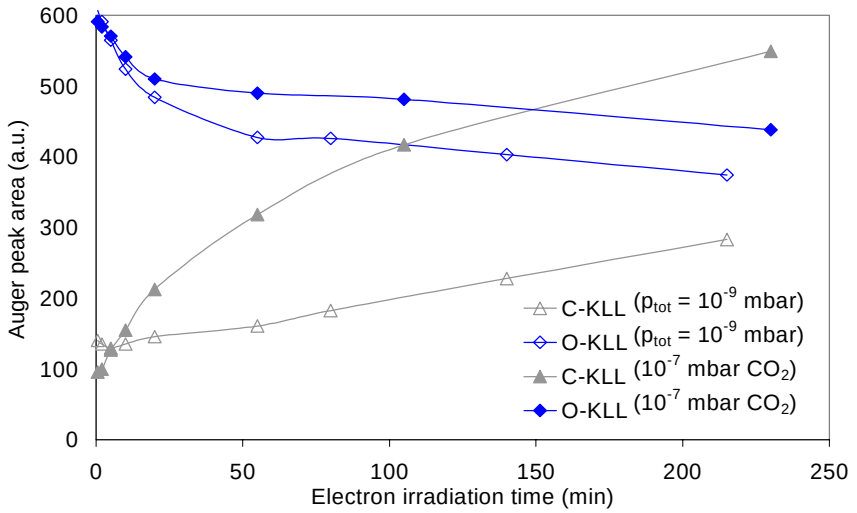

Figure 6: Variation of the C-KLL and O-KLL Auger peak intensities as a function of electron irradiation time at a total pressure $p_{tot} = 10^{-9}$ mbar and during simultaneous CO_2 injection at 10^{-7} mbar. The substrate is a TiZrV coating as received after deposition and 1 h air exposure.

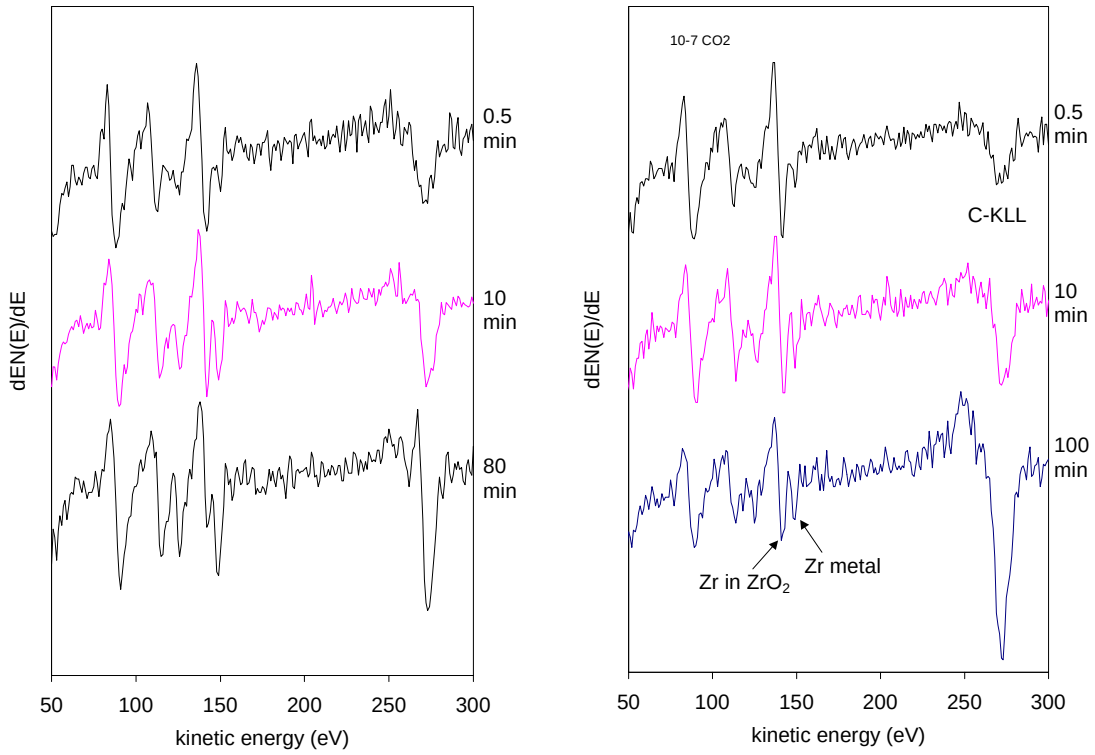

Figure 7: Characteristic zirconium and carbon peaks in the derivative dEN(E)/dE Auger electron spectra after different e^- irradiation times without gas injection (left plot) and during 10^{-7} mbar CO_2 injection (right plot). The Zr-MNV peak at 142 eV is characteristic for Zr in ZrO_2 and the peak at 147 eV is characteristic for Zr metal.

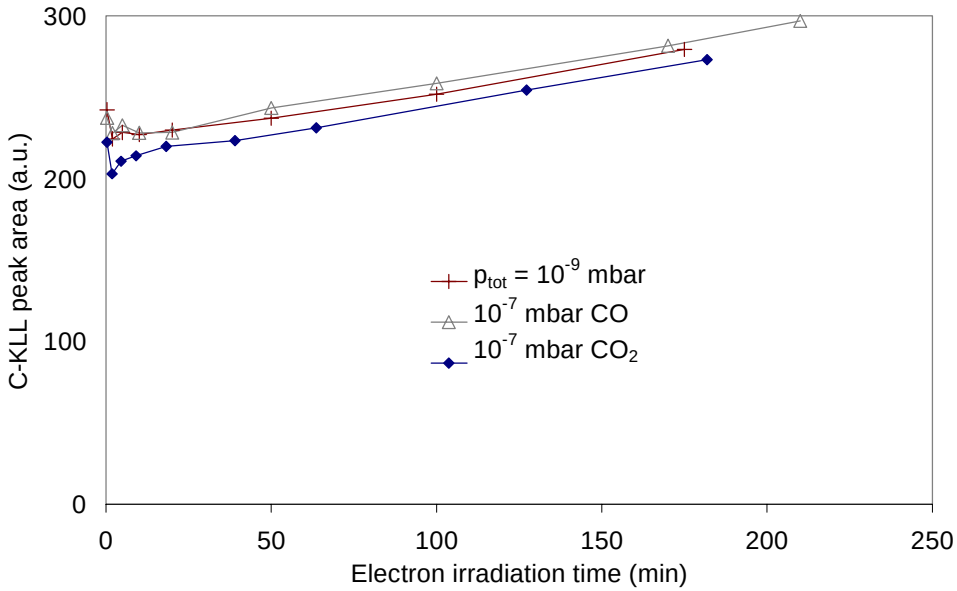

Figure 8: Variation of the C-KLL intensity as a function of electron dose on a copper substrate at different CO and CO_2 pressures. Before the measurements the copper sample has been chemically cleaned and exposed to air.